Radiation Physics and Chemistry 215 (2024) 111368

Contents lists available at ScienceDirect

Radiation Physics and Chemistry

journal homepage: www.elsevier.com/locate/radphyschem

Design of beam line for BNCT applications in HEC-1 channel of IRT-T research reactor

S. Bagherzadeh-Atashchi [a], N. Ghal-Eh [a,*], F. Rahmani [b], R. Izadi-Najafabadi [a], S.V. Bedenko [c]

[a] Department of Physics, Faculty of Science, Ferdowsi University of Mashhad, P.O. Box 91775-1436, Mashhad, Iran
[b] Department of Physics, K. N. Toosi University of Technology, P.O. Box 16315-1618, Tehran, Iran
[c] School of Nuclear Science and Engineering, Tomsk Polytechnic University, P.O. Box 634050, Tomsk, Russian Federation

ARTICLE INFO

Handling Editor: Dr. Chris Chantler

Keywords:
Boron Neutron Capture Therapy (BNCT)
IRT-T research reactor
Beam Shaping Assembly (BSA)
Neutron converter
In–phantom parameters

ABSTRACT

The feasibility of using the HEC-1 beam port of the IRT-T research reactor to generate an epithermal neutron beam for Boron Neutron Capture Therapy (BNCT) was investigated using MCNPX2.6 Monte Carlo simulation. The reactor was first simulated to design and optimize a Beam Shaping Assembly (BSA) that meets the neutron beam criteria recommended by the International Atomic Energy Agency (IAEA). The suggested BSA configuration consisted of a cylindrical geometry with 25 cm of MgF_2 and 15 cm of Fluental® as a moderator, 15 cm of Pb as a reflector, two 5 cm Bi slabs as gamma-ray shields, and 4 mm of ^{6}Li and 5 mm of borated polyethylene sheets as thermal neutron filters. The results showed that the epithermal neutron flux at the BSA exit was 2.3×10^9 n/cm^2.s, and in-phantom dose analysis indicated that the designed beam could be used for the treatment of deep brain tumors within an allowable treatment time of 50 min.

1. Introduction

Boron Neutron Capture Therapy (BNCT) is a promising tumor treatment method that operates on the principle of delivering thermal neutrons to cancer cells that contain a significant amount of ^{10}B, which has a high neutron absorption cross-section. This results in higher neutron absorption in tumor cells than in healthy tissue with a lower ^{10}B concentration. When ^{10}B absorbs neutrons, it produces high-energy ^{7}Li and α particles that can deposit their energy into tumor cells, leading to their destruction. The Q-value of $^{10}B(n_{th}, \alpha)^7Li$ reaction is 2.31 MeV which is converted to the kinetic energies of α (1.47 MeV) and ^{7}Li (0.84 MeV) particles (Seppälä et al., 1999; Torres-Sánchez et al., 2019; Macías et al., 2021).

During treatment, it is crucial to confirm that healthy tissues receive a lower dose due to their lower concentration of ^{10}B. However, these unwanted doses must still be lower than the maximum allowable value. To ensure the quality of treatment, two sets of criteria must be met: the criteria for the beam's performance in the phantom and the criteria for the beam before reaching the tissue. The IAEA has recommended a set of parameters, known as in-air parameters, that can be used as criteria to design the beam for BNCT (IAEA-TECDOC-1223, 2001). To provide an appropriate neutron beam, a Beam Shaping Assembly (BSA) must be designed based on the neutron source specifications. Nuclear research reactors and accelerators are the primary sources of neutrons for BNCT (Herrera et al., 2013; Kreiner, 2012; Allen and Beynon, 1995; Wang et al., 2014; Kasesaz et al., 2014a; Kasesaz et al., 2014b; Bortolussi et al., 2018; Rahmani and Shahriari, 2011; Ghal-Eh et al., 2017). In this study, the IRT-T research reactor was used as a neutron source, and an appropriate neutron beam was designed based on the HEC-1 port facility using the MCNPX2.6 code (Pelowitz, 2008).

2. Materials and methods

2.1. IRT-T reactor

The IRT-T is a 6 MW (thermal neutron - 1.7×10^{14} n/cm^2.s; fast neutrons - 2.0×10^{13} n/cm^2.s), pool-type research reactor that uses beryllium as a reflector, demineralized water as a coolant/moderator and has a top biological shield. The reactor design has 56 in-core positions with 7.15 cm of lattice pitch for fuel assemblies and reflector blocks. The reactor core consists of 12 eight-tube and 8 six-tube fuel assemblies of the IRT-3M type, which contain highly enriched uranium fuel plates in the form of UO_2–Al alloy. The height and thickness of fuel meat are 58 and 0.04 cm, respectively and the thickness aluminum

* Corresponding author.
E-mail address: ghal-eh@um.ac.ir (N. Ghal-Eh).

https://doi.org/10.1016/j.radphyschem.2023.111368
Received 15 June 2023; Received in revised form 20 September 2023; Accepted 24 October 2023
Available online 27 October 2023

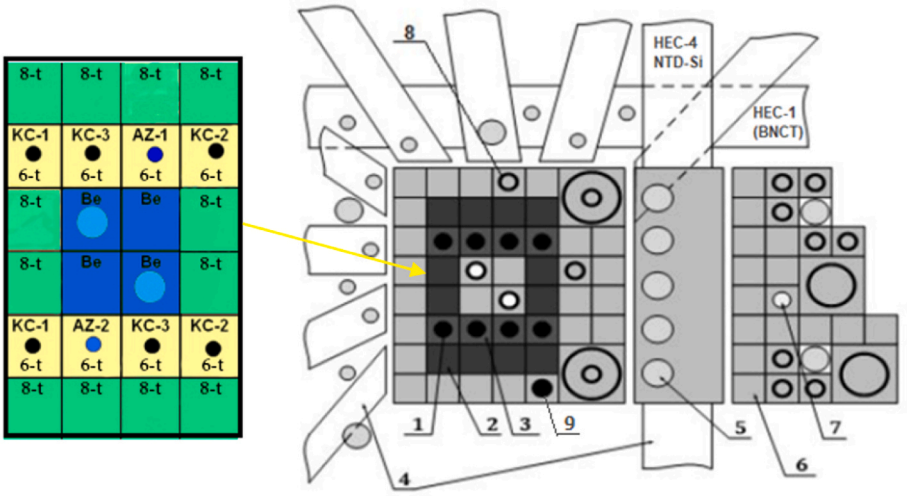

Fig. 1. IRT-T reactor core, 1: Control rods, 2: 8-tube fuel assemblies (8-t), 3: 6-tube fuel assemblies (6-t), 4: HEC, 5: VEC, 6: Beryllium blocks (Be), 7: Experimental channels with water, 8: Experimental channels in peripheral beryllium, 9: Regulating rod (AR) in Beryllium block, KC-1, KC-2 KC-3: Shim rod, AZ-1, AZ-2, AZ-3: Scram rod.

cladding is 0.05 cm (Glukhov and Didenko, 1988; Gradoboev et al., 2021; Shchurovskaya et al., 2016). Fig. 1 provides a visual representation of the reactor core and its main components. The IRT-T reactor has 14 vertical experimental channels (VECs) and 10 horizontal beam tubes (HECs), respectively, including 8 radial beam ports with a diameter of 100 mm, 2 tangents of 150 mm diameter, and a beryllium thermal column. The reactor has nine control rods, which include three groups of shim rods (KS-1, KS-2, and KS-3 with two rods per group), two scram rods (AZ-1 and AZ-2), and one regulating rod (AR). The control rods are positioned at the center of the 6-tube fuel assemblies, except for the regulating rod, which is placed at the center of the beryllium block (Chertkov et al., 2021).

The MCNPX2.6 code was used to create a detailed model of the reactor, including experimental components, fuel assemblies, control rods, beryllium, some vertical experimental channels, and two radial tangent beam ports (HEC-1 and HEC-4). Fig. 2(a) and (b) show a cross-section of the model using the MCNPX2.6 viewer.

A comparative analysis of the beam parameters obtained at IRT-T was conducted with those of the Tehran Research Reactor (TRR) and other similar facilities. TRR is a 5 MW reactor using U_3O_8–Al MTR type fuel whilst light water is used as moderator, coolant, and shielding. The results of investigation in (Kasesaz et al., 2014a) showed that epithermal neutron flux at the exit of the BSA in the thermal column can be used for BNCT.

In order to validate the simulation, the results from Anikin et al. were utilized for comparison. Anikin's study focused on the feasibility of using the IRT-T research reactor for designing a thermal neutron beam for BNCT applications.

2.2. BSA design

The design of BSA was performed using the MCNPX2.6 code, as shown in Fig. 3. The major parts of the BSA include a neutron converter (Faghihi and Khalili, 2013; Harling et al., 2002; Sauerwein et al., 2012; Mokhtari et al., 2017), moderator, thermal neutron filter, reflector, collimator, and gamma-ray filter. The IRT-T neutron energy spectrum and its specifications, the BSA materials, and the geometry were optimized based on the recommended IAEA parameters.

Moderators used in BNCT typically have a high scattering cross-section for fast neutrons and a low absorption cross-section for epithermal neutrons. Several commonly used moderators include Al, AlF_3, Al_2O_3, Fe, TiF_3, MgF_2, Al/AlF_3 alloy (30% Al, 70% AlF_3), and Fluental® alloy (30% Al, 69% AlF_3, 1% LiF). In the preliminary stage, the above moderators with different lengths in cylindrical geometry were examined.

Next, a thermal neutron filter was added to eliminate thermal neutrons from the epithermal neutron beam. ^{6}Li and borated polyethylene sheets were used at the beginning and end of the selected moderators to minimize thermal neutron contribution to the beam (Fig. 3).

A suitable reflector was then added. Lead is a commonly used reflector material, and different thicknesses were tested for each moderator.

Finally, a collimator was inserted in the beamline, and a gamma-ray shield was optimized to reduce the gamma-ray dose to the desired value. The collimator was designed to converge the therapeutic neutron beam at the exit window and had a shape of an incomplete cone shell with larger and smaller radii of 35 and 5 cm surrounded by Pb. The collimator length was optimized to obtain maximum epithermal neutron flux at the exit. To reduce the gamma-ray dose, two Bi slabs were added at the beginning and end of the moderator, and a Bi layer was included on the interior surface of the collimator. For all BSA designs, thermal, epithermal, and fast neutron flux, as well as the epithermal to total neutron flux ratio, were calculated.

2.3. Evaluation of in-phantom parameters

The in-phantom parameters for the computational Snyder head phantom model were calculated to evaluate the performance of the epithermal neutron beam (Snyder et al., 1969). These parameters include AD (Advantage Depth), ADDR (Advantage Depth Dose Rate), TD (Therapeutic Depth), and TT (Treatment Time). AD is the depth at which the dose to the tumor equals the maximum dose to the normal tissue, ADDR is the maximum dose rate to normal tissue, TD is the depth at which the tumor dose falls below twice the maximum dose to normal tissue, and TT is defined as the time that dose delivered to normal tissue exceeds the maximum tolerated dose (12.5 RBE-Gy). The Snyder head phantom model is defined by equation (1) (dimensions in cm), consisting of three ellipsoids that divide the head into three regions of skin, skull, brain, and a spherical tumor at the center (Fig. 4).

$$\begin{aligned}\left(\frac{x}{6.0}\right)^2+\left(\frac{y}{9.0}\right)^2+\left(\frac{z}{6.5}\right)^2&=1\ (\text{Brain})\\ \left(\frac{x}{6.8}\right)^2+\left(\frac{y}{9.8}\right)^2+\left(\frac{z}{8.3}\right)^2&=1\ (\text{Skull})\\ \left(\frac{x}{7.3}\right)^2+\left(\frac{y}{10.3}\right)^2+\left(\frac{z}{8.8}\right)^2&=1\ (\text{Skin})\end{aligned} \quad (1)$$

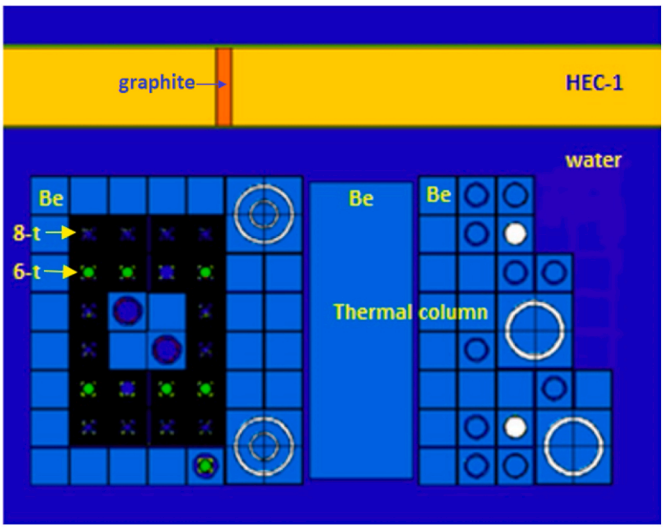

(a)

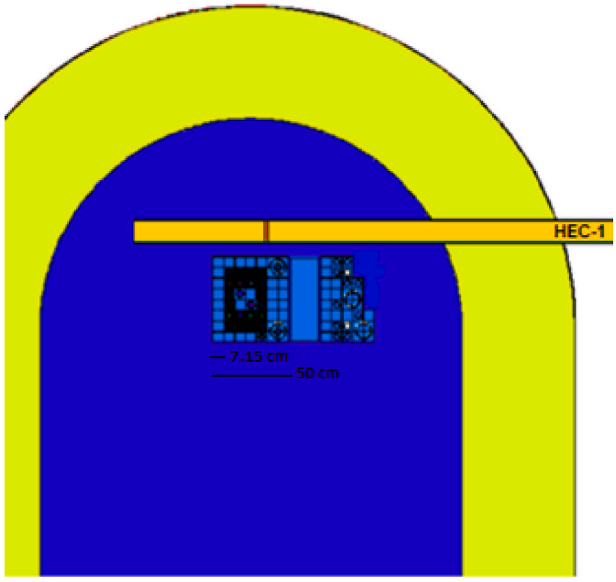

(b)

Fig. 2. IRT-T reactor core as simulated by MCNPX2.6 (a) Horizontal section, (b) Total view.

The elemental composition of phantom material was based on the ICRU 46 (ICRU Report 46, 1992). The weighted total dose (D_w) is defined as the sum of physical dose components multiplied by the weighting factors of each dose component in a tissue:

$$D_w = w_B D_B + w_N D_N + w_{fn} D_{fn} + w_g D_g \quad (2)$$

where, D_g is the gamma-ray dose, D_B is the absorbed dose due to the boron, D_N is the nitrogen dose, and D_{fn} is the fast neutron dose. The ratio of ^{10}B concentration in the normal tissue to that in the tumor is 18:65. The weighting factors w_N and w_{fn} are equally assumed as 3.2, w_g is 1.0, and w_B values are 1.3, 2.5, and 3.8 in the normal tissue, skin, and tumor, respectively (Zamenhof et al., 1975; Coderre et al.,1993; Torres-Sanchez et al., 2021). The four dose components were individually calculated along the beam's central axis through the brain using flux-to-dose conversion factors, as specified in (ICRU Report 46, 1992), in conjunction with F4 tally and DE4/DF4 cards in the MCNPX code. To assess the variation of different dose components as a function of phantom depth, 46 equal-sized rectangular 1.6 × 1.6 × 0.4 cm^3 voxels were considered (Fig. 4) and F4 tally was calculated in each voxel.

3. Results and discussion

3.1. Neutron and gamma-ray energy spectra of HEC-1 beam port

Neutron and gamma-ray spectra in the HEC-1 beam port were calculated and are illustrated in Figs. 5 and 6. Relative statistical errors are less than 2% for thermal neutrons, 10% for epithermal neutrons, and 8% for fast neutrons as well as 10% for gamma-rays, respectively.

Neutron flux in three energy groups for the HEC-1 beam port is listed

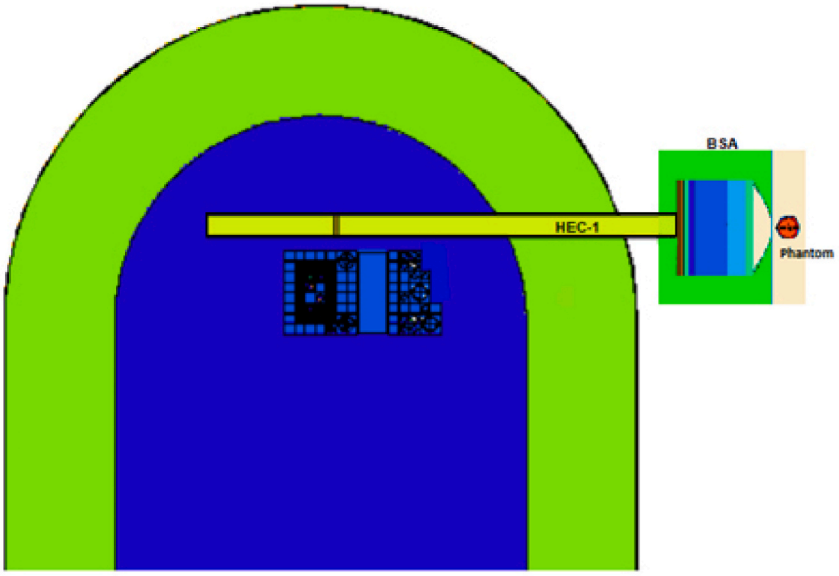

(a)

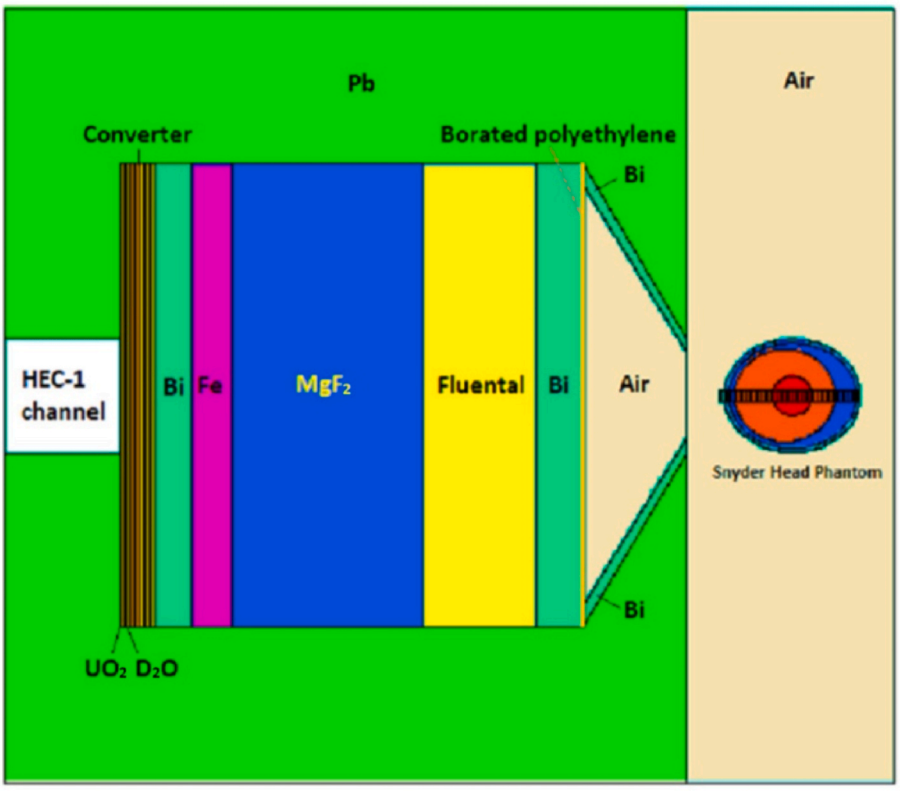

(b)

Fig. 3. (a) Total view with BSA, (b) The designed BSA.

in Table 1 and these results are compared with Anikin et al.'s (Fig. 7). Despite the consistency of data in both studies, it should be noted that only HEC-1 and HEC-4 channels were simulated in Anikin's research, so there may be some slight variations between the results.

3.2. Beam shaping assembly

One of the main objectives of the present study is to reduce the fast and thermal neutron as well as gamma-ray dose rates as much as possible while maintaining the epithermal neutron flux above 1.0×10^9 n/cm^2.s. For this purpose, first, a 5 cm-thick iron slab was placed in front of the exit of the IRT-T reactor HEC-1 channel. This particular thickness was obtained from the removal cross-section data for converting fast neutrons to an energy of about 100 keV. Then, seven moderators with different thicknesses were used in order to decrease the neutron beam energy down to the epithermal region. It should be noted that the moderator thickness can be increased to such an extent that the flux does not decrease too much, therefore thicknesses up to 40 cm were examined.

Figs. 8 and 9 show the variations of Φ_{epi}, and Φ_{epi}/Φ_{fast}, against

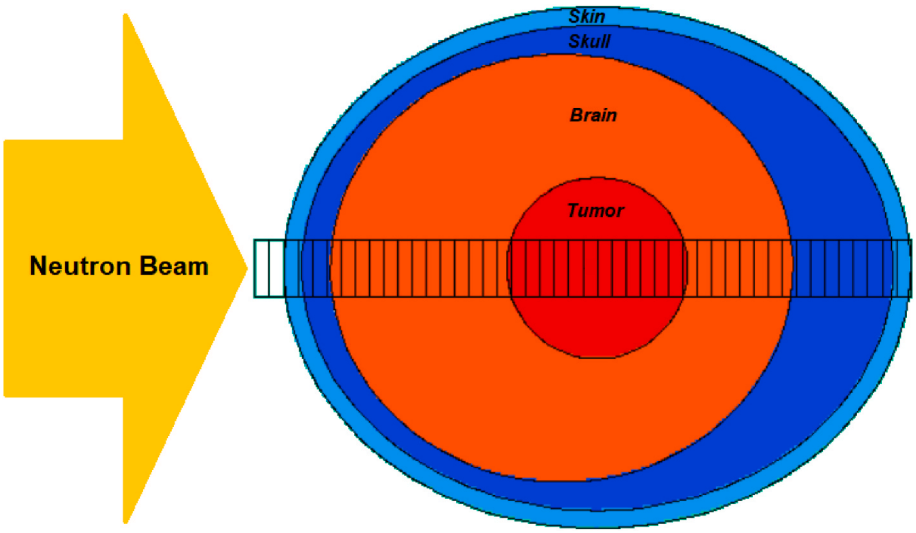

Fig. 4. Snyder head phantom containing three ellipsoids corresponding to skin, skull, brain, and also a central sphere as a tumor.

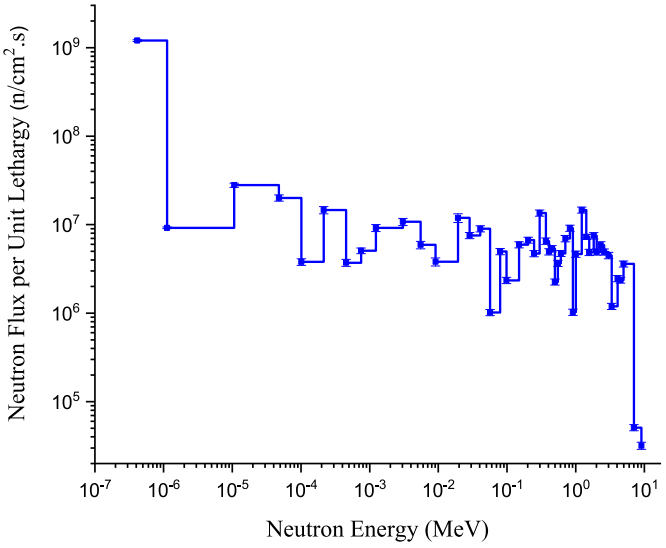

Fig. 5. Neutron energy spectrum at the exit of HEC-1 channel.

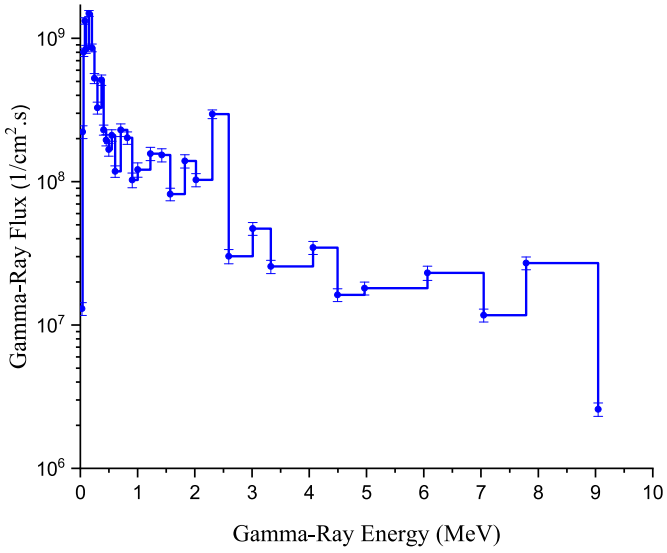

Fig. 6. Gamma-ray energy spectrum at the exit of HEC-1 channel.

moderator thickness. The moderators that provide the highest value of Φ_{epi}, and Φ_{epi}/Φ_{fast} are Fluental® and MgF_2. Then different thicknesses of these two moderators were considered as the primary and secondary moderators. The best result in this stage was obtained with 25 cm of MgF_2 as the primary and 15 cm of Fluental® as the secondary moderators.

Variation of epithermal neutron flux as a function of reflector thickness was also considered. The best value of epithermal neutron flux was achieved by adding a 20 cm Pb reflector surrounding the moderators.

The results of adding two thermal neutron filters at the beginning and the end of moderators have been considered. A 4-mm thick ^{6}Li sheet and 2-mm thick borated polyethylene were selected as the primary and secondary thermal neutron filters, respectively.

Since a 50-cm long collimator has the smallest proportion of non-epithermal neutron flux, it has been chosen as the best collimator length. Moreover, to reduce the gamma-ray dose, a 3-cm Bi layer over the interior surface of the collimator, a 5-cm thick Bi slab at the beginning, and a 6-cm thick Bi slab at the end of moderators have been selected as gamma-ray filters.

Table 1
Neutron fluxes in 3 energy groups at the exit of HEC-1 beam port.

Neutron flux component (n/cm².s)	This study	Anikin et al. (2020)
Thermal	8.70×10^8	8.41×10^8
Epithermal	7.84×10^7	1.07×10^8
Fast	1.28×10^8	1.28×10^8

The general idea of the neutron converter function is to use neutron flux (originating from the core center) to initiate new fission reactions of ^{235}U in uranium plates which results in fast neutron generation. In this study, a neutron converter has been used to provide the necessary epithermal neutron flux for the BNCT in the IRT-T research reactor, which consists of uranium oxide plates, 90% enriched in ^{235}U. To enhance the number of neutrons at the BSA entrance, the converter containing five uranium plates, each with a thickness of 0.4 cm, was used. The converter is located at the end of the HEC-1 channel. The 0.4-cm thick D_2O has been used between uranium oxide plates as a coolant. Table 2 summarizes the neutron fluxes in three energy groups at the BSA exit, with and without the neutron converter.

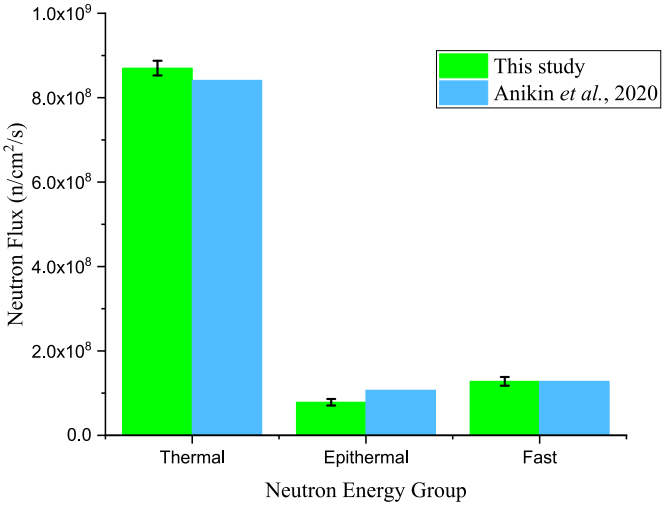

Fig. 7. HEC-1 neutron flux.

Table 2
Different energy groups of neutron flux with and without neutron converter at the BSA exit.

Neutron flux component (n/cm^2.s)	Without converter	With converter
Thermal	1.14×10^7	1.06×10^8
Epithermal	1.90×10^8	2.33×10^9
Fast	1.18×10^7	2.10×10^8

All neutron beam parameters for the final configuration have been calculated and presented in comparison to IAEA-recommended values in Table 3. We made a comparison between the IRT-T designed beam and findings from previously published studies in Table 3. The neutron spectrum related to the designed BSA configuration is shown in Fig. 10. The figure demonstrates that the neutron spectrum designed for IRT-T exhibits a favorable range of epithermal energies, with high neutron flux.

3.3. *In-phantom parameters*

Figs. 11 and 12 show the neutron and photon fluxes in all 46 different

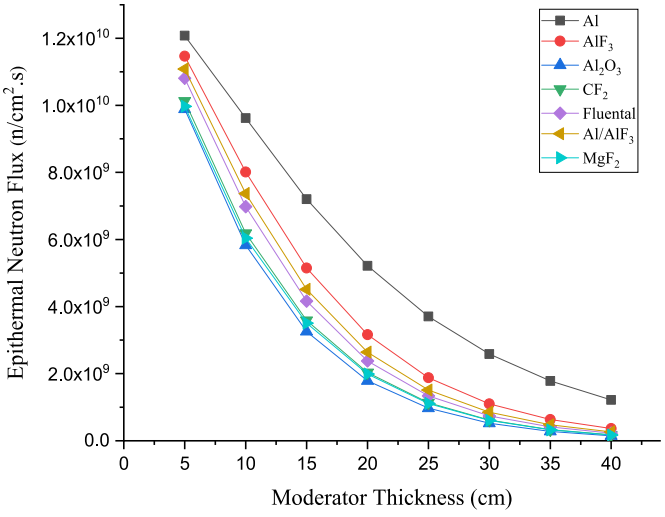

Fig. 8. Variation of epithermal neutron flux vs. moderator length.

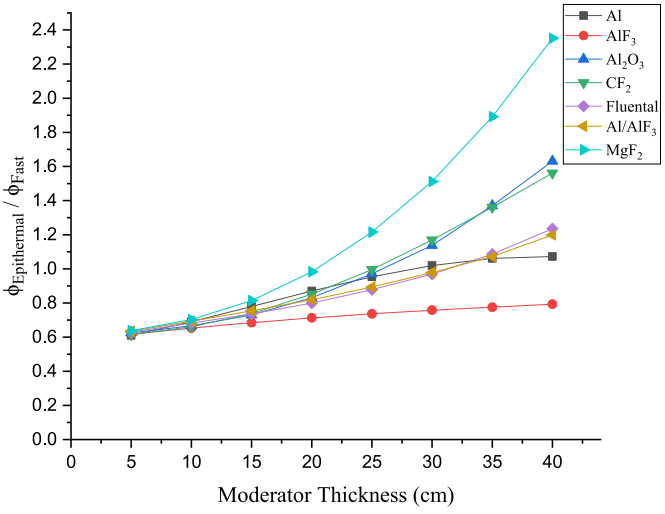

Fig. 9. Variation of Φ_{epi}/Φ_{fast} vs. moderator thickness.

Table 3
Comparison of neutron beam parameters of IRT-T current design and other facilities.

	IAEA limit	IRT-T	TRR (Kasesaz et al., 2014a)	THOR (Liu et al., 2004)	FiR-1 (Binns et al., 2002)	R2-0 (Binns et al., 2002)	Syrian MNSR (Shaaban and Albarhoum, 2015)	Isfahan MNSR (Monshizadeh et al., 2015)
Φ_{th} (n/cm^2.s)		1.06×10^8						
Φ_{epi} (n/cm^2.s)	$>1 \times 10^9$	2.33×10^9	0.65×10^9	1.69×10^9	1.2×10^9	1.43×10^9	0.28×10^9	0.635×10^9
Φ_f (n/cm^2.s)		2.10×10^8						
$\dot{D}_f/\Phi_{epi}$ (Gy.cm^2)	$<2 \times 10^{-13}$	1.9×10^{-13}	2.2×10^{-13}	2.8×10^{-13}	3.3×10^{-13}	8.3×10^{-13}	7.98×10^{-13}	0.07×10^{-13}
$\dot{D}_\gamma/\Phi_{epi}$ (Gy.cm^2)	$<2 \times 10^{-13}$	4.9×10^{-13}	2.1×10^{-13}	1.25×10^{-13}	0.9×10^{-13}	12.6×10^{-13}	1.7×10^{-13}	0.87×10^{-13}
Φ_{th}/Φ_{epi}	$<5 \times 10^{-2}$	4.4×10^{-2}	4×10^{-2}				5×10^{-2}	7×10^{-3}

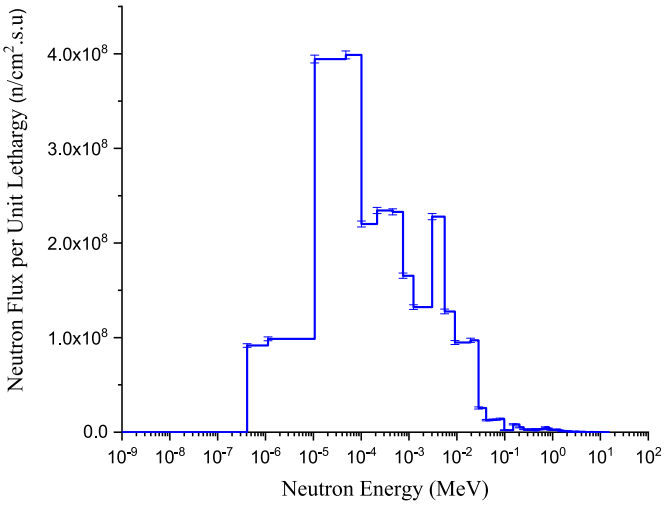

Fig. 10. Neutron energy spectrum at the beam port of the final BSA configuration.

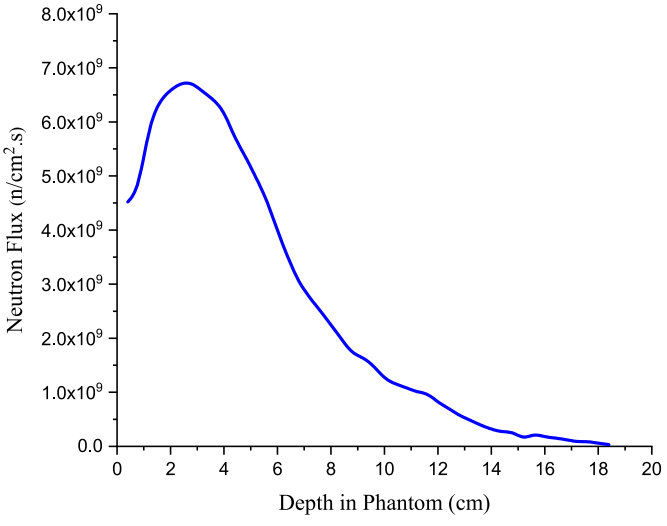

Fig. 11. Variation of neutron flux against the depth in phantom.

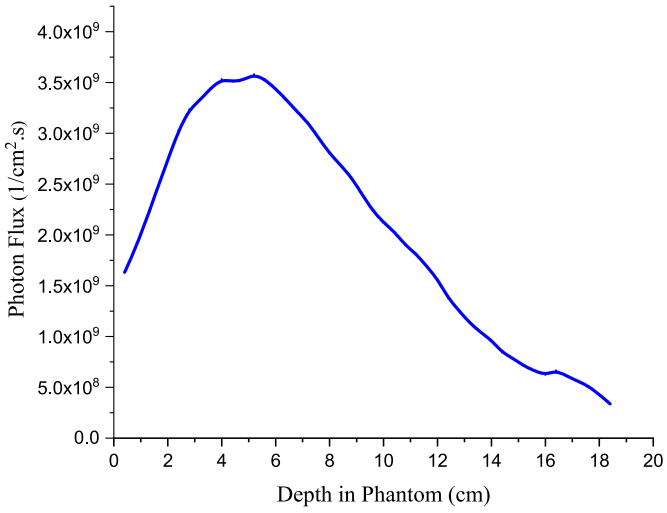

Fig. 12. Variation of photon flux against the depth in phantom.

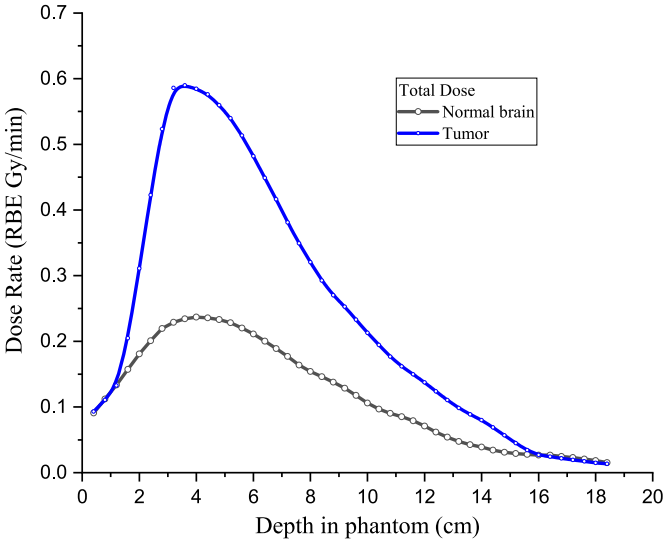

Fig. 13. Variation of depth dose against the depth in phantom.

rectangular voxels specified in the head phantom, which have been calculated as a function of discrete energies by the MCNPX code. The variations of total depth dose versus phantom depth when the whole phantom is filled with either healthy tissue or tumor material have been shown in Fig. 13. As discussed in Section 2.3, the major in–phantom parameters include ADDR, AD, TD, and TT. The in-phantom parameters corresponding to the final epithermal BSA are reported in Table 4 in

Table 4
In-phantom parameters calculated for Snyder head phantom compared with some published works (Tumor: Normal tissue ^{10}B concentration (ppm) = 65:18).

	IRT-T	TRR (Kasesaz et al., 2014a)	FiR-1 (Binns et al., 2002)	Syrian MNSR (Shaaban and Albarhoum, 2015)	Isfahan MNSR (Monshizadeh et al., 2015)
ADDR (cGy/min)	24.7	49	45	9	18
AD (cm)	9.1	7.5	9	7.5	8.4
TD (cm)	6	4.9	5.8	–	6.8
TT (min)	50	25	30	135	70

comparison to some published works. The table indicates that the designed BSA enables deep penetration of the therapeutic beam, as evidenced by its high AD value.

4. Conclusions

An epithermal neutron beam has been designed based on the IRT-T reactor neutron source. A BSA including neutron converter, moderator, reflector, filters, and collimator has been proposed for the HEC-1 channel of IRT-T. According to our calculations with the MCNP2.6 code, the designed epithermal neutron beam is suitable for BNCT applications. Calculated in-phantom parameters show that the designed beam can be used for the treatment of deep-seated brain tumors in 50 min which is an allowable time. The results confirm that the IRT-T reactor has a good potential to be considered as a pilot for the BNCT research facility.

In the next phase of this research study, the proposed BSA will be equipped with the ThErmal Neutron Imaging System (TENIS) (Yazdandoust et al., 2021) to enable real-time neutron spectroscopy and imaging for the quality assurance of the therapeutic beam.

Credit author statement

Somayyeh Bagherzadeh-Atashchi: Software, Visualization, Writing., ***Nima Ghal-Eh***: Supervision, Methodology, Visualization, Conceptualization, Writing., ***Faezeh Rahmani***: Supervision, Methodology, Visualization, Conceptualization, Writing., ***Reza Izadi-Najafabadi***: Methodology, Writing, Visualization, Conceptualization., ***Sergey V. Bedenko***: Methodology, Writing, Visualization, Conceptualization.

Declaration of competing interest

The authors declare that they have no known competing financial interests or personal relationships that could have appeared to influence the work reported in this paper.

Data availability

Data will be made available on request.

Acknowledgments

This work was supported by grant N⁰ 3/55605 (28/06/1400) from the Vice President for Research and Technology of Ferdowsi University of Mashhad. Authors are also grateful to the center of TPU's "Physical and Chemical Methods of Analysis".

References

Allen, D.A., Beynon, T.D., 1995. A design study for an accelerator-based epithermal neutron beam for BNCT. Phys. Med. Biol. 40 (5), 807.
Anikin, M.N., Lebedev, I.I., Naymushin, A.G., Smolnikov, N.V., 2020. Feasibility study of using IRT-T research reactor for BNCT applications. Appl. Radiat. Isot. 166, 109243.
Binns, P.J., Riley, K.J., Harling, O.K., 2002. Dosimetric comparison of six epithermal neutron beams using an ellipsoidal water phantom. Res. Dev. Neutron Capture Ther. 405–409.
Bortolussi, S., Protti, N., Ferrari, M., Postuma, I., Fatemi, S., Prata, M., Ballarini, F., Carante, M.P., Farias, R., González, S.J., Marrale, M., 2018. Neutron flux and gamma dose measurement in the BNCT irradiation facility at the TRIGA reactor of the University of Pavia. Nucl. Instrum. Methods Phys. Res. Sect. B Beam Interact. Mater. Atoms 414, 113–120.
Chertkov, Y.B., Anikin, M.N., Lebedev, I.I., Naimushin, A.G., Smol'nikov, N.V., 2021. Calculation and experimental determination of the neutronics characteristics of the IRT-T research reactor. Atom. Energy 131 (1), 42–45.
Coderre, J.A., Makar, M.S., Micca, P.L., Nawrocky, M.M., Liu, H.B., Joel, D.D., Slatkin, D. N., Amols, H.I., 1993. Derivations of relative biological effectiveness for the high-LET radiations produced during boron neutron capture irradiations of the 9L rat gliosarcoma in vitro and in vivo. Int. J. Radiat. Oncol. Biol. Phys. 27 (5), 1121–1129.
Faghihi, F., Khalili, S., 2013. Beam shaping assembly of a D–T neutron source for BNCT and its dosimetry simulation in deeply-seated tumor. Radiat. Phys. Chem. 89, 1–13.
Ghal Eh, N., Goudarzi, H., Rahmani, F., 2017. FLUKA simulation studies on in–phantom dosimetric parameters of a LINAC–based BNCT. Radiat. Phys. Chem. 141, 36–40.
Glukhov, G.G., Didenko, A.N., 1988. The IRT-T reactor at tomsk polytechnical institute nuclear physics research institute: research and applications. Sov. Atom. Energy 64 (5), 423–426.
Gradoboev, A.V., Bondarenko, E.A., Varlachev, V.A., Yemets, E.G., Sednev, V.V., 2021. A Technique for Studying the Resistance of LEDS to Irradiation by Fast Neutrons at the IRT-T Reactor. Instruments and Experimental Techniques, vol. 64, pp. 619–622. Naymushin, A., Anikin, M., Lebedev, I., Busygin, A., Dmitriev, S. and Zolotykh, D., 2016. Features of fuel burnup calculations for IRT-T reactor using MCU-PTR code. Journal of Industrial Pollution Control, 32(2), pp.449–452.
Harling, O.K., Riley, K.J., Newton, T.H., Wilson, B.A., Bernard, J.A., Hu, L.W., Fonteneau, E.J., Menadier, P.T., Ali, S.J., Sutharshan, B., Kohse, G.E., 2002. The fission converter-based epithermal neutron irradiation facility at the Massachusetts Institute of Technology reactor. Nucl. Sci. Eng. 140 (3), 223–240.
Herrera, M.S., González, S.J., Minsky, D.M., Kreiner, A.J., 2013. Evaluation of performance of an accelerator-based BNCT facility for the treatment of different tumor targets. Phys. Med. 29 (5), 436–446.
IAEA-TECDOC-1223, 2001. Current Status of Neutron Capture Therapy.
International Commission on Radiation and Measurements ICRU, 1992. Photon, Electron, Proton and Neutron Interaction Data for Body Tissues. ICRU.
Kasesaz, Y., Khalafi, H., Rahmani, F., 2014a. Design of an epithermal neutron beam for BNCT in thermal column of Tehran research reactor. Ann. Nucl. Energy 68, 234–238.
Kasesaz, Y., Khalafi, H., Rahmani, F., Ezati, A., Keyvani, M., Hossnirokh, A., Shamami, M. A., Monshizadeh, M., 2014b. A feasibility study of the Tehran research reactor as a neutron source for BNCT. Appl. Radiat. Isot. 90, 132–137.
Kreiner, A.J., 2012. Accelerator-based BNCT. *Neutron Capture Therapy: Principles and Applications*, pp. 41–54.
Liu, Y.W., Huang, T.T., Jiang, S.H., Liu, H.M., 2004. Renovation of epithermal neutron beam for BNCT at THOR. Appl. Radiat. Isot. 61 (5), 1039–1043.
Macías, M., Fernández, B., Praena, J., 2021. New data for the definition of neutron beams for Boron Neutron capture therapy. Radiat. Phys. Chem. 185, 109474.
Mokhtari, J., Faghihi, F., Khorsandi, J., Hadad, K., 2017. Conceptual design study of the low power and LEU medical reactor for BNCT using in-tank fission converter to increase epithermal flux. Prog. Nucl. Energy 95, 70–77.
Monshizadeh, M., Kasesaz, Y., Khalafi, H., Hamidi, S., 2015. MCNP design of thermal and epithermal neutron beam for BNCT at the Isfahan MNSR. Prog. Nucl. Energy 83, 427–432.
Pelowitz, D.B., 2008. User's Manual, Version of MCNPX2. 6.0, 672 LANL, LA-CP-07-1473.
Rahmani, F., Shahriari, M., 2011. Beam shaping assembly optimization of Linac based BNCT and in-phantom depth dose distribution analysis of brain tumors for verification of a beam model. Ann. Nucl. Energy 38 (2–3), 404–409.
Sauerwein, W.A., Wittig, A., Moss, R., Nakagawa, Y. (Eds.), 2012. Neutron Capture Therapy: Principles and Applications. Springer Science & Business Media.
Seppälä, T., Vähätalo, J., Auterinen, I., Kosunen, A., Nigg, D.W., Wheeler, F.J., Savolainen, S., 1999. Modelling of brain tissue substitutes for phantom materials in neutron capture therapy (NCT) dosimetry. Radiat. Phys. Chem. 55 (3), 239–246.
Shaaban, I., Albarhoum, M., 2015. Design calculation of an epithermal neutronic beam for BNCT at the Syrian MNSR using the MCNP4C code. Prog. Nucl. Energy 78, 297–302.
Shchurovskaya, M.V., Alferov, V.P., Geraskin, N.I., Radaev, A.I., Naymushin, A.G., Chertkov, Y.B., Anikin, M.N., Lebedev, I.I., 2016. Control rod calibration simulation using Monte Carlo code for the IRT-type research reactor. Ann. Nucl. Energy 96, 332–343.
Snyder, W.S., Ford, M.R., Warner, G.G., Fisher Jr., H.L., 1969. Estimates of Absorbed Fractions for Monoenergetic Photon Sources Uniformly Distributed in Various Organs of a Heterogeneous Phantom. Oak Ridge National Lab., Tenn.
Torres-Sánchez, P., Porras, I., de Saavedra, F.A., Sabariego, M.P., Praena, J., 2019. On the upper limit for the energy of epithermal neutrons for Boron Neutron Capture Therapy. Radiat. Phys. Chem. 156, 240–244.
Torres-Sanchez, P., Porras, I., de Saavedra, F.A., Praena, J., 2021. Study of the upper energy limit of useful epithermal neutrons for Boron Neutron Capture Therapy in different tissues. Radiat. Phys. Chem. 185, 109490.
Wang, L.W., Chen, Y.W., Ho, C.Y., Liu, Y.W.H., Chou, F.I., Liu, Y.H., Liu, H.M., Peir, J.J., Jiang, S.H., Chang, C.W., Liu, C.S., 2014. Fractionated BNCT for locally recurrent

head and neck cancer: experience from a phase I/II clinical trial at Tsing Hua open-pool reactor. Appl. Radiat. Isot. 88, 23–27.
Yazdandoust, H., Ghal-Eh, N., Firoozabadi, M.M., 2021. TENIS—ThErmal neutron imaging System for use in BNCT. Appl. Radiat. Isot. 176, 109755.
Zamenhof, R.G., Murray, B.W., Brownell, G.L., Wellum, G.R., Tolpin, E.I., 1975. Boron neutron capture therapy for the treatment of cerebral gliomas. I: theoretical evaluation of the efficacy of various neutron beams. Med. Phys. 2 (2), 47–60.